Spin-resonant splitting in magnetically modulated semimagnetic semiconductor superlattices

Yong Guo

Department of Physics, Tsinghua University, Beijing 100084, People's Republic of China

Jun-Qiang Lu and Bing-Lin Gu

Centre for Advanced Study, Tsinghua University, Beijing 100084, People's Republic of China

Yoshiyuki Kawazoe

Institute for Materials Research, Tohoku University, Sendai 980-8577, Japan

We investigate spin-resonant splitting in magnetically modulated semimagnetic semiconductor superlattices by adopting tight-binding model and Green's function method under the influence of an external electric field. Spin-dependent resonant splitting features for both the transmission spectra and the current density spectra are discussed in more detail. Under no influence of the external electric field, the periodic nature of the spin superlattice leads to a regular profile of quantization in the transmission, which is composed of spin-dependent resonant bands separated by nonresonant gaps, where the resonant splitting rule of the transmission for spin-up case is exactly the same as that for spin-down case. The transmission resonances are drastically suppressed by the external electric field, the difference between resonant bands and nonresonant gaps is lessened and the transmission spectra are smoothed out. It is shown that splitting of the current density is more complex. In contrast with the transmission, the number of oscillations in the current density spectra has no simple direct correspondence to the number of unit cells and cannot be summarized in the simple rule.

I. INTRODUCTION

Recently the nascent field of ''spintronics'' has attracted considerable attention.[1−28] It is expected that the spintronics may herald a conceptual revolution in electronics: one that exploits the spins of electrons, rather than their charges. Single spin is considered as the ultimate limit of information storage.[1] In the applications, the spin of the electron has been taken into consideration for the design of new quantum devices, such as spin quantum computers,[2] spin-memory devices,[3] spin transistors,[4] spin filters and modulators, and so on. However, none of these devices exist yet, and experimental progress as well as theoretical investigation are needed to provide guidance and support in the search for realizable implementations. Further, most of the proposed spintronic devices involve spin-polarized transport across interfaces in various hybrid structures, such as magnetic tunnel junctions,[12] diluted magnetic semiconductor heterostructures,[13] ferromagnetic semiconductor heterostructures,[14] semiconductor-superconductor hybrid structures,[15] etc. Ortenberg[16] theoretically proposed the spin-superlattice, which was experimentally realized by Dai *et al.*[17] and by Chou *et al.*,[18] respectively. After that many creative theoretical and experimental works have been done by exploiting spin-dependent phenomena. Sugakov and Yatskevich[19] examined spin splitting in parallel electric and magnetic fields through a double-barrier heterojunction using a transfer-matrix method. Recently, Egues[20] theoretically investigated electronic spin filtering in perpendicular transport through a tunable ZnSe/Zn$_{1-x}$Mn$_x$Se heterostructure with a single paramagnetic layer. The results indicate a strong suppression of the spin-up component of the current density while increasing magnetic fields and the total current density is dominated by the spin-down component for $B > 2$ T. The reason is that in an external magnetic field the paramagnetic layer of the heterostructure behaves as a potential well for spin-down electrons and a potential barrier for spin-up ones. The study further showed that the electric field can greatly change the status of polarization of the tunneling electron in the semimagnetic semiconductor heterostructure with a single paramagnetic layer.[21] Interesting spin-resonant suppression and enhancement are found in the semimagnetic semiconductor heterostructures with double paramagnetic layers,[22] that are originated from the combined effects introduced by the structural symmetry and asymmetry as well as the applied electric field. Experimentally, there has achieved great progress in transporting a spin-polarized current across the interface between two semiconductors-one magnetic and one nonmagnetic. Fiederling *et al.*[23] experimentally used the magnetic semiconductor zinc selenide doped with beryllium and manganese Be$_x$Mn$_y$Zn$_{1-x-y}$Se and reported the injection of spin-polarized electrons. Ohno *et al.*[24] used manganese-doped GaAs and have seen polarized hole injection into a light-emitting diode. In both cases, the researchers passed their spin-polarized current into a GaAs-based light-emitting diode, with an efficiency of about 90 and 2 %, respectively. Jonker and his co-workers[25,26] have performed similar experiments using paramagnetic ZnMnSe as the spin aligner and observed about 50% optical polarization. Further, a model for the ferromagnetism of GaMnAs is developed and the Curie temperatures for other Mn-doped semiconductors are predicted.[27] Very recently there has achieved a significant advance towards the realization of multifunctional semiconductor spintronics by Malajovich *et al.*[28] They studied GaAs/ZnSe heterostructures as building blocks for semiconductor spintronics and find that the efficiency for

injecting spin from GaAs to ZnSe is significantly enhanced by applying an electrical bias. These noticeable results imply that fully switchable all-semiconductor spin valves should be feasible.

It is well known that features for electron tunneling through superlattices are quite different from that for electron tunneling through single-barrier or single-well heterostructures. One important feature exhibited in periodic superlattices is the resonant splitting effect, in which resonant peaks split with increasing the number of building blocks. This feature is closely related with minibands and minigaps of eigenenergy structures. The effects were first demonstrated numerically in the pioneering work by Tsu and Esaki.[29] It was found that a resonance peak of transmission in a double-barrier electric structure splits into a doublet in a triple-barrier electric structure and quadruplets in a quintuple-barrier structure. Liu and Stamp[30,31] went further by investigating the general case in which the semiconductor superlattice are modeled by periodically arranged potential barriers and wells both with arbitrary profiles. Resonant splitting features through semiconductor superlattices which are periodically juxtaposed with two different barriers are also generalized.[32] Further, Guo and his co-workers[33] first investigated resonant splitting effects in periodic magnetic superlattices, in which similarities and differences of splitting features through electrically modulated superlattices and magnetically modulated superlattices are presented. Later, Zeng et al.[34] generalized the resonant splitting features for ballistic conductance peaks in magnetically periodic superlattices. Although there has been a few of work on resonant splitting in periodic electric or magnetic superlattices, some basic questions are still unclear. A few interesting questions we raise here are (1) does resonant splitting occur for electron tunneling through multiple-well structures? If it occurs, what is the splitting rule? (2) How does the external electric field affect the resonant splitting in periodic superlattices? (3) What splitting features are for measurable quantity (i.e., the current density)? Are they the same as that for the transmission or not? All of the above questions are very basic and should be clarified.

In the present paper we investigate spin resonant splitting effects on electron tunneling through magnetically modulated ZnSe/Zn$_{1-x}$Mn$_x$Se spin superlattices. The potential of the corresponding superlattice is both spin dependent and field induced. In an external magnetic field the paramagnetic layers of the superlattice behave as potential wells for spin-down electrons and potential barriers for spin-up ones. Therefore, this kind of spin superlattice is an ideal system for simultaneously investigating resonant splitting in multiple-well as well as multiple-barrier structures. Moreover, a better understanding of the spin resonant splitting properties of magnetically modulated ZnSe/Zn$_{1-x}$Mn$_x$Se spin superlattices might bring useful insights into its possible applications in microelectronics and optoelectronics.

This article is organized as follows. In Sec. II we present a brief description of the tight-binding model and the real space Green's function method. The calculated results are given in Sec. III with analyses. In Sec. IV, the concluding remarks are summarized.

II. MODEL AND FORMULAS

In Mn-based semimagnetic semiconductor systems electrons interact with the $3d$ electrons of the localized magnetic moments of the Mn ions via the sp-d exchange interaction. For a conduction electron, this exchange interaction can be written as Heisenberg type Hamiltonian $H_{\text{int}} = -\Sigma_i J(\vec{r} - \vec{R}_i)\vec{S} \cdot \vec{S}_i$, where $\vec{r}$ and $\vec{S}$ are, the position and the spin of the conduction electron, R_i and S_i are positions and spins of i numbers Mn^{2+} ions, respectively. Within typical approximations, it allows to calculate energy states of conduction and valence electrons by $k \cdot p$ perturbation method. The $k \cdot p$ matrix is augmented by diagonal terms which for the conduction band are equal to $A = N_0\alpha\sigma_z x\langle S_z\rangle$, where N_0 is the number of unit cells per unit volume, $\alpha = \langle\Psi|J|\Psi\rangle$ is the exchange integral, parameter of interaction of electrons with Mn^{2+} ions, σ_z is the electron spin components $\pm 1/2$ (or $\uparrow, \downarrow$) along the field, x is the mole fraction of Mn, and $\langle S_z\rangle$ is the thermal average of zth component of Mn^{2+} spin (a 5/2 Brillouin function).

Because of the sp-d exchange interaction, an external magnetic field applied to the ZnSe/Zn$_{1-x}$Mn$_x$Se system modulates the potential profile ''seen'' by a traversing electron (or heavy hole) in a spin-dependent fashion. Spin-down electrons see a multiple-well potential while spin-up ones see a multiple-barrier potential. Here in Sec. II, we constrict our theoretical analyses to the magnetically modulated spin superlattice, which is a periodic arrangement with one Zn$_{1-x}$Mn$_x$Se layer and one ZnSe layer. The formalism obtained can be naturally extended to the more complex superlattice, which is periodically arranged with three different layers. Within mean field and for a magnetic field along the z axis, the sp-d exchange interaction gives rise to a spin-dependent potential

$$V_{\sigma_z} = -N_0\alpha\sigma_z x\langle S_z\rangle \sum_n \{\Theta[z-(n-1)L_1$$
$$-(n-1)L_2]\Theta[nL_1+(n-1)L_2-z]\} \qquad (1)$$

in the Hamiltonian of the system. Here, $\Theta(z)$ is the Heaviside function, L_1 and L_2 are the widths of Zn$_{1-x}$Mn$_x$Se paramagnetic layer and ZnSe layer, respectively. Under an applied bias V_a along the z axis, an electric-field-induced term $-eV_a z/L_t$ ($L_t = nL_1 + nL_2$) should be added to the potential. The Hamiltonian of an electron in the framework of the parabolic-band effective-mass approximation can be written as

$$\hat{H}_{xy} = \frac{1}{2m_e^*}[\hat{P}_x^2 + (\hat{P}_y + eBx)^2], \qquad (2)$$

$$\hat{H}_z = \frac{1}{2m_e^*}\hat{P}_z^2 + V_{\sigma_z}(z) - \frac{eV_a z}{L_t}. \qquad (3)$$

In the absence of any kind of electron scattering the motion along the z axis is decoupled from that of the x-y plane. The in-plane motion is quantized in Landau levels with energies $E_n = (n+1/2)\hbar\omega_c$, where $n = 0, 1, 2, \ldots$, and ω_c

$=eB/m_e^*$ (we assume a single electron mass m_e^* throughout the spin superlattice). Therefore, the motion of the electrons can be reduced to one-dimensional problem along the z axis. In the following we adopt the tight-binding model and the real space Green's function method and present formulas for the transmission coefficient, the density of states, and the current density.

Within the tight-binding formalism, we can model the reduced one-dimensional motion in ZnSe/Zn$_{1-x}$Mn$_x$Se spin superlattices by the following Hamiltonian:

$$H_z = \sum_{i\sigma_z} \varepsilon_{i\sigma_z} \alpha_{i\sigma_z}^\dagger \alpha_{i\sigma_z} - \sum_{ii'\sigma_z} V \alpha_{i\sigma_z}^\dagger \alpha_{i'\sigma_z}, \qquad (4)$$

where the sum over lattice sites i and i' is restricted to nearest neighbors, $V = \hbar^2/2m_e^* a^2$ is the hopping integral and set its value equal to one as the energy unit.

The transmission coefficients through the system can be obtained from the real space Green's function and temperature Kubo formula[35] as

$$
\begin{aligned}
T_{\sigma_z}&(E_z, B, V_a) \\
&= \frac{2a^2}{L_z^2} \mathrm{Tr}[\tilde{G}_{\sigma_z}(j,j')\tilde{G}_{\sigma_z}(j'-1,j-1) \\
&\quad + \tilde{G}_{\sigma_z}(j-1,j'-1)\tilde{G}_{\sigma_z}(j',j) - \tilde{G}_{\sigma_z}(j,j'-1) \\
&\quad \times \tilde{G}_{\sigma_z}(j',j-1) - \tilde{G}_{\sigma_z}(j-1,j')\tilde{G}_{\sigma_z}(j'-1,j)], \qquad (5)
\end{aligned}
$$

where

$$\tilde{G}_{\sigma_z}(j,j') = [G_{\sigma_z}(E_z+i\varepsilon;j,j') + G_{\sigma_z}(E_z-i\varepsilon;j,j')]/2i$$

with G_{σ_z} is the matrix element of the real space Green's function. Note that the transmission coefficients are functions of the incident energy E_z, the magnetic field B, and the applied bias V_a.

The spin-dependent density of states (SDOS) ρ_{σ_z} is related to the Green's function of a whole system via a standard formula

$$\rho_{\sigma_z}(E_z, B, V_a) = -\frac{1}{\pi} \lim_{\varepsilon \to 0^+} \mathrm{Im}\{\mathrm{Tr}G_{\sigma_z}(E_z+i\varepsilon)\}. \qquad (6)$$

This expression allows the SDOS to be calculated as a function of the electron energy E_z as well as the external fields B and V_a for a system with multiple layers.

We assume that the ZnSe layers are emitter and collector attached to external leads. The average spin-dependent current density is defined by

$$
\begin{aligned}
I_{\sigma_z}(B,V_a) = e &\sum_{n,k_y,k_z \geqslant 0} v_z(k_z) T_{\sigma_z}(E_z, B, V_a) \\
&\times \{f[E_z+(n+\tfrac{1}{2})\hbar\omega_c] \\
&\quad - f[E_z+(n+\tfrac{1}{2})\hbar\omega_c+eV_a]\} \int |\psi_{n,k_y,k_z}|^2 dv,
\end{aligned}
$$
$$(7)$$

where $\psi_{n,k_y,k_z} = (1/\sqrt{L_y})(1/\sqrt{L_z}) e^{ik_y y} e^{ik_z z} \varphi_n(x)$. Here, $\varphi_n(x)$ is the nth harmonic-oscillator eigenfunction centered at $x_0 = -\hbar k_y/m\omega_c$, k_y and k_z are the electron wave vectors along the y and z directions, f is the Fermi-Dirac distribution function. These scattering states have energies $E_{n,k_z} = (n+\tfrac{1}{2})\hbar\omega_c + \hbar^2 k_z^2/2m_e^*$. The summation on k_y is equal to $L_x L_y eB/2\pi\hbar$, $\varphi_n(x)$ is normalized. Therefore, Eq. (7) becomes

$$
\begin{aligned}
J_{\sigma_z}(B,V_a) = J_0 B &\sum_{n=0}^{\infty} \int_0^{+\infty} T_{\sigma_z}(E_z, B, V_a) \\
&\times \{f[E_z+(n+\tfrac{1}{2})\hbar\omega_c] \\
&\quad - f[E_z+(n+\tfrac{1}{2})\hbar\omega_c+eV_a]\} dE_z, \qquad (8)
\end{aligned}
$$

where $J_0 = e^2/4\pi^2\hbar^2$.

In the absence of the applied magnetic field, the conduction and valence band offsets in ZnSe/Ze$_{1-x}$Mn$_x$Se heterostructures are nearly zero (see Fig. 1 in Ref. 20), i.e., $V_{\sigma_z} \approx 0$. At this case, the difference of electronic transport between spin-up electrons and spin-down electrons disappeared, thus transport through the superlattice becomes spin-independent and no longer possesses spin-filtering features.

When $T = 0$ K, the above equation reduces to

$$J_{\sigma_z}(B,V_a) = J_0 B \sum_{n=0}^{n_{\max}} \int_0^{E_f-(n+1/2)\hbar\omega_c} T_{\sigma_z}(E_z, B, V_a) dE_z,$$
$$eV_a > E_f, \qquad (9)$$

$$J_{\sigma_z}(B,V_a) = J_0 B \sum_{n=0}^{n_{\max}} \int_{E_0}^{E_f-(n+1/2)\hbar\omega_c} T_{\sigma_z}(E_z, B, V_a) dE_z,$$
$$eV_a < E_f, \qquad (10)$$

where $n_{\max}(B) = \mathrm{int}[(E_f-E_z)/\hbar\omega_c - \tfrac{1}{2}]$, $E_0 = [E_f-(n+\tfrac{1}{2})\hbar\omega_c - eV_a]\Theta[E_f-(n+\tfrac{1}{2})\hbar\omega_c - eV_a]$ and Θ is the step function. For B going to infinity, a 5/2 Brillouin function reaches to 1, thus the spin-dependent potential introduced by the sp-d exchange interactions V_{σ_z} becomes $-5/2xN_0\alpha\sigma_z$. Therefore, the difference of the effective potential "seen" by the spin up electrons and by the spin-down ones reach maximal, which results in the largest degree of the spin polarization. To evaluate the electron spin-polarization effect, it is useful to calculate the spin polarization of the transmitted beam, which can be defined by

$$P(B,V_a) = \frac{J_\uparrow(B,V_a) - J_\downarrow(B,V_a)}{J_\uparrow(B,V_a) + J_\downarrow(B,V_a)}, \qquad (11)$$

where $J_\uparrow$ and $J_\downarrow$ are the current density for spin-up and spin-down electrons, respectively.
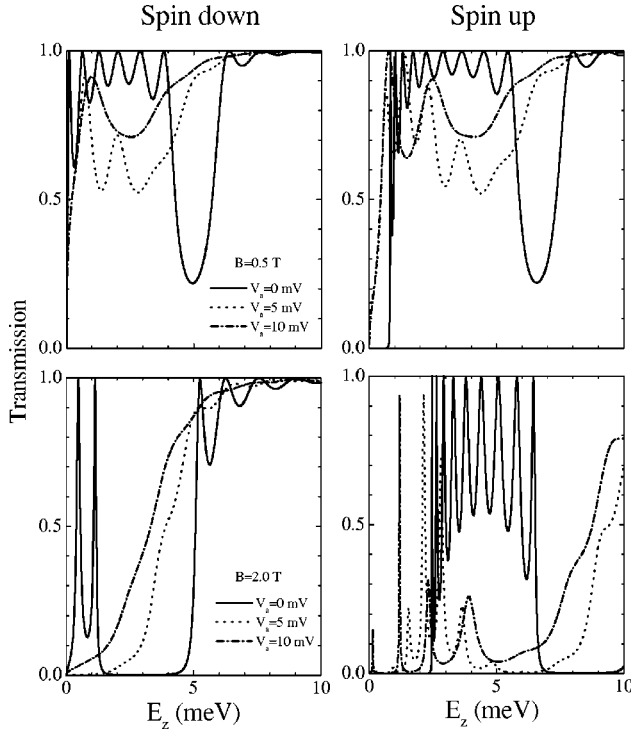
FIG. 1. Spin-dependent transmission coefficients for spin-up and spin-down electrons traversing one ZnSe/Zn$_{1-x}$Mn$_x$Se spin superlattice at zero bias and under two fixed applied biases V_a = 5,10 mV. $L_1 = L_2 = 10$ nm, $B = 0.5,2$ T.

III. RESULTS AND ANALYSES

In this section we discuss spin resonant splitting in the magnetically modulated ZnSe/Zn$_{1-x}$Mn$_x$Se spin superlattice. Three different configurations of spin superlattices are considered. First one is a periodic arrangement of Zn$_{1-x}$Mn$_x$Se layer A and ZnSe layer B in sequence of $ABAB$, where two building layers have same widths $L_1 = L_2 = 10$ nm. Second one is a periodic arrangement of Zn$_{1-x}$Mn$_x$Se layer A and ZnSe layer B with different widths, where $L_1 = 20$ nm is for the Zn$_{1-x}$Mn$_x$Se building layer, $L_2 = 10$ nm is for the ZnSe building layer. Third one is a periodic arrangement of two Zn$_{1-x}$Mn$_x$Se layers A and C (with different widths $L_1 = 20$ nm and $L_3 = 10$ nm, respectively) and one ZnSe layer B (with width $L_2 = 10$ nm), in which the arrangement is in sequence of $ABCBABCB$. Electrons in Mn-based systems interact with the $3d$ electrons of the localized magnetic moments of the Mn ions via the sp-d exchange interaction. The concentration of Mn in the paramagnetic layer is chosen so that in the absence of an applied magnetic field, the conduction and valence band offsets are nearly zero. In an external magnetic field the sp-d exchange interaction gives rise to a giant spin splitting ΔE_s which exceed both the Laudau level splitting $\hbar \omega_c$ and the thermal energy $k_B T$,[36] which lifts the degeneracy of the spin-up and spin-down electron and hole states. The paramagnetic layer in the ZnSe/Zn$_{1-x}$Mn$_x$Se spin superlattice behaves as a well potential for spin-down electrons and a barrier potential for spin-up ones. Thus, in our considered semimagnetic semiconductor systems, spin-up electrons see a multiple-barrier potential while spin-down ones see a multiple-well potential. When we adjust the widths of building layers, or apply an external electric field to the system, or change the strength of the applied magnetic field, the effective potential "seen" by electrons is changed correspondingly. Therefore, there should exist rich and interesting spin-dependent tunneling features in our considered system.

In Fig. 1 spin-dependent transmission coefficients are plotted as functions of the incident energy E_z along the z direction for electron traversing a ZnSe/Zn$_{1-x}$Mn$_x$Se spin superlattice at zero bias and under two fixed applied biases. Two building layers Zn$_{1-x}$Mn$_x$Se and ZnSe have same widths $L_1 = L_2 = 10$ nm. The total number of repeat unit is equal to ten (i.e., $n = 10$). In all of the graphs, we use $m_e^* = 0.16 m_e$ (m_e is the mass of free electron), an effective Mn concentration $x_{\text{eff}} = x(1-x)^{12}$ with $x = 0.05$, $N_0 \alpha = 0.26$ eV, and $T = 4.2$ K. The external magnetic field is set to be $B = 0.5$ T and $B = 2.0$ T for calculation and discussion. The corresponding magnitudes of spin-dependent potential V_{σ_z} are 1.6127 and 5.3235 meV, respectively. One can easily see that the former potential is much less than the latter one. From the following discussion (see Figs. 9 and 10), one can also see that at $B = 0.5$ T, the difference between the spin-up component and the spin-down one of the current density is smaller, thus the degree of the spin polarization is low. Generally, the spin polarization is always less than 0.5 (i.e., $P < 0.5$) for $B = 0.5$ T, while for $B = 2$ T the spin polarization is larger than 0.5 in the wide range of the applied bias (i.e., $P > 0.5$). Here we would like to point out that in this sense $B = 0.5$ T is a small magnetic field while $B = 2.0$ T is a large one. In the superlattice considered in Fig. 1, for spin-up electrons, the magnetic-induced potential at zero bias is ten identical barriers, which are separated by nine identical wells, while for spin-down ones, the potential is multiple wells, which have ten identical wells. At zero bias, one can easily see that resonant bands are formed in the transmission spectra, which are separated by nonresonant gaps. As the external magnetic field increases, the width of the resonant band is strongly narrowed. Further, tunneling through this system exhibits noticeable spin-dependent features. For spin-up electrons, the position and width of each resonant band as well as the space distance between adjacent resonant peaks are quite different from those for spin-down electrons. However, the resonant splitting rule is same for both cases, that is, for n-barrier or n-well tunneling, splitting is always $(n-1)$-fold. Under the influence of an external electric field, the resonant-band structure of the transmission spectra is strongly modified. Resonances are suppressed, the resonant regions are smoothed out and enlarged, and distances between adjacent peaks are widened. For a larger applied bias, it is difficult to distinguish resonant bands and gaps, even to sum up a simple rule to describe main features of splitting for the transmission coefficient.

When we increase the width of building paramagnetic layer (see Fig. 2), the typical feature is that resonant splitting rule for the transmission is not changed. The band structure is still apparent for both spin-up case and spin-down case. For larger magnetic fields, the transmission tends to zero in the gaps, while in the band region the transmission exhibits a resonant behavior. However, the width of each resonant band
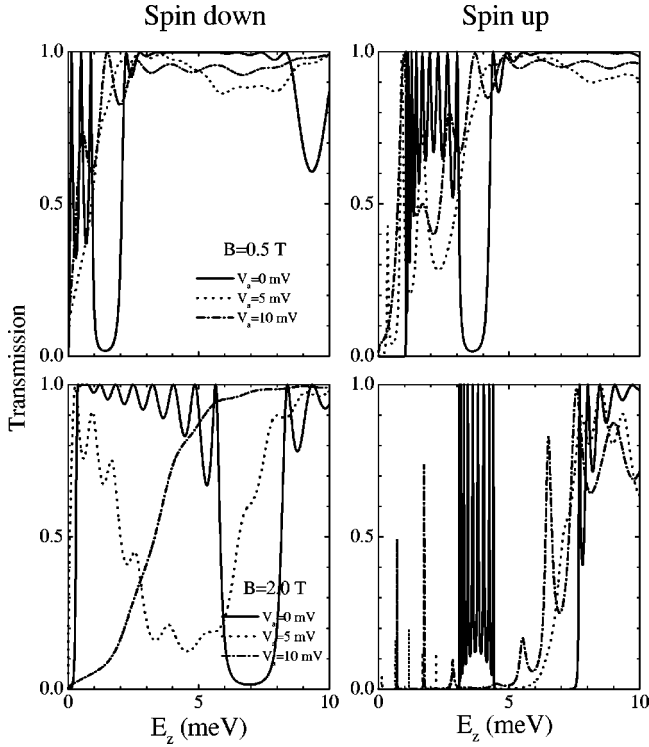
FIG. 2. Spin-dependent transmission coefficients for spin-up and spin-down electrons traversing one ZnSe/$Zn_{1-x}Mn_xSe$ spin superlattice at zero bias and under two fixed applied biases V_a = 5,10 mV. L_1 = 20 nm, L_2 = 10 nm, B = 0.5,2 T.

FIG. 3. Spin-dependent transmission coefficients for spin-up and spin-down electrons traversing one ZnSe/$Zn_{1-x}Mn_xSe$ spin superlattice at zero bias and under two fixed applied biases V_a = 5,10 mV. L_1 = 20 nm, L_2 = 10 nm, L_3 = 10 nm, B = 0.5,2 T.

is strongly narrowed while forbidden gaps are strongly broadened. Figure 3 shows that transmission coefficients for electron tunneling through the third configuration of superlattice, which is periodically arranged by one ZnSe layer (with width L_2 = 10 nm) and two $Zn_{1-x}Mn_xSe$ layers (with widths L_1 = 20 nm and L_3 = 10 nm). In comparison with the resonant band structures of last two configurations exhibited in Figs. 1 and 2, resonant bands further split, that is, each one resonant band in the former splits into two resonant subbands in the latter. For both spin-up case and spin-down case, each subbands consists of equal number of resonant peaks, and each peak has unity value at zero bias. The results once again strongly indicate that at zero bias or under the influence of a smaller bias, the resonant splitting rule obtained from periodic multiple-barrier structures is applicable to periodic multiple-well structures.

As is well known, for electron tunneling through the electric semiconductor superlattice, when the incident energy of electrons coincides with the energy of bound states in the potential well, the resonant tunneling occurs. Because of the coupling between the wells via tunneling through the barriers of finite width, the degenerate eigenlevels of the independent wells are split, consequently, these split levels redistribute themselves into groups around their unperturbed positions and form quasibands. This leads to the resonant splitting of transmission. As the number of periods (or the number of barriers) tends to infinity, the locally continuous energy distribution (energy band) is formed. Here we would like to point out that the basic feature of the formation of minibands
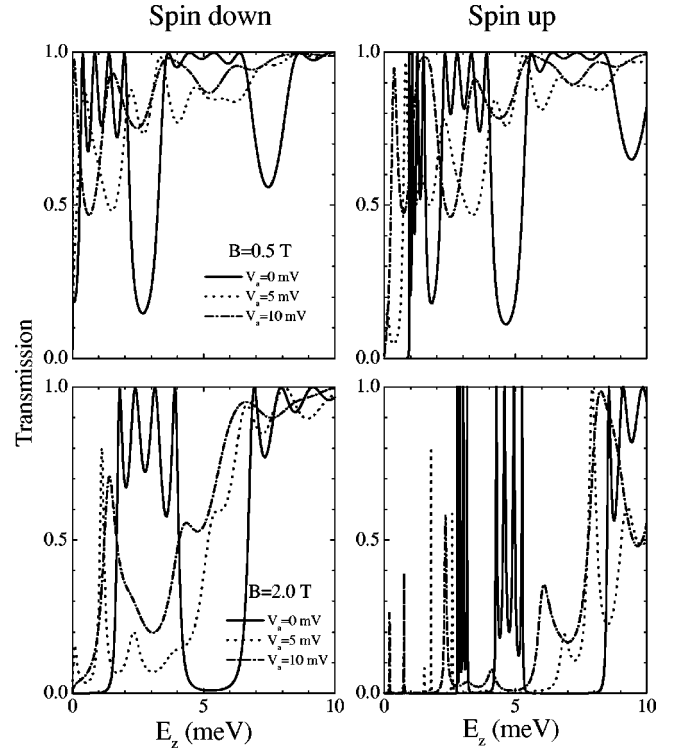
and gaps are observable for a periodic superlattice with even a few periods. Further, for our considered spin superlattice, the spacing between adjacent resonant peaks can be quantum-size induced and magnetic-field induced. We should also notice that the quasibound state energies of an infinite-well potential is $E_n = n^2 \hbar^2 \pi^2 / 2m_e^* L^2$ (here L is the width of the infinite well). Both eigenenergies E_n of quasibound states and the spacing $\Delta = (2n-1)\hbar^2 \pi^2 / 2m_e^* L^2$ between adjacent quasibound energy levels are determined by the length of the width of the well. The larger the length, the lower are the eigenenergies of bound states. The spacing between adjacent eigenstates is narrowed correspondingly. As the magnetic field increases, the corresponding well becomes deeper, the distance between adjacent levels is reduced. Bear these in mind, we can easily understand the spin-dependent as well as size- and field-induced features exhibited in Figs. 1–3.

Many important physical properties and characteristics of a system with multilayers are determined by the density of states. In order to help readers better understand the spin-dependent features exhibited in Figs. 1–3, from Figs. 4–6 we present the relative SDOS distribution within the structure for three different configurations of magnetically modulated ZnSe/$Zn_{1-x}Mn_xSe$ spin superlattices. The configuration and parameters for Figs. 4, 5, and 6 are exactly the same as those for Figs. 1, 2, and 3, respectively. We see that at zero bias the SDOS distribution exhibits oscillations bands and nonoscillation bands. In the low incident energy range, oscillations become more rapid and the magnitudes of the oscil-
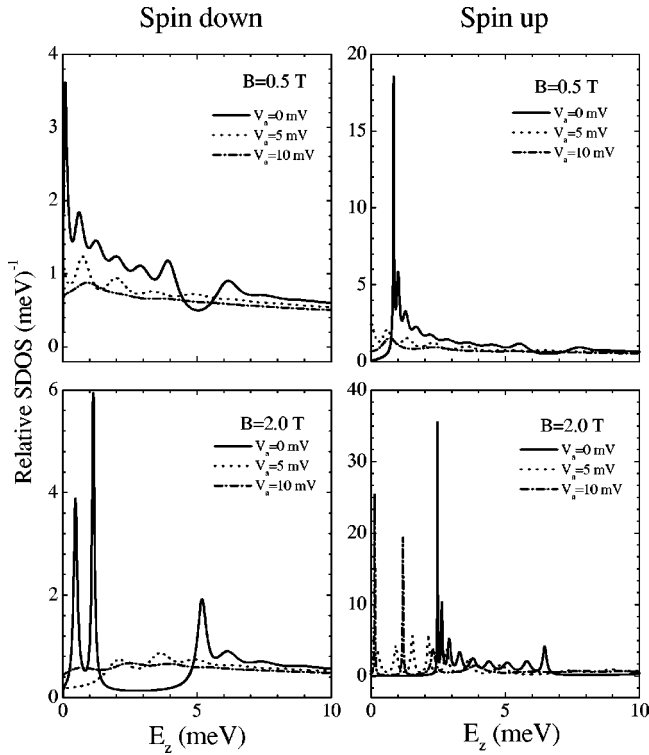
FIG. 4. The relative SDOS distribution within one ZnSe/$Zn_{1-x}Mn_x$Se spin superlattice at zero bias and under two fixed applied biases $V_a = 5, 10$ mV. $L_1 = L_2 = 10$ nm, $B = 0.5, 2$ T.
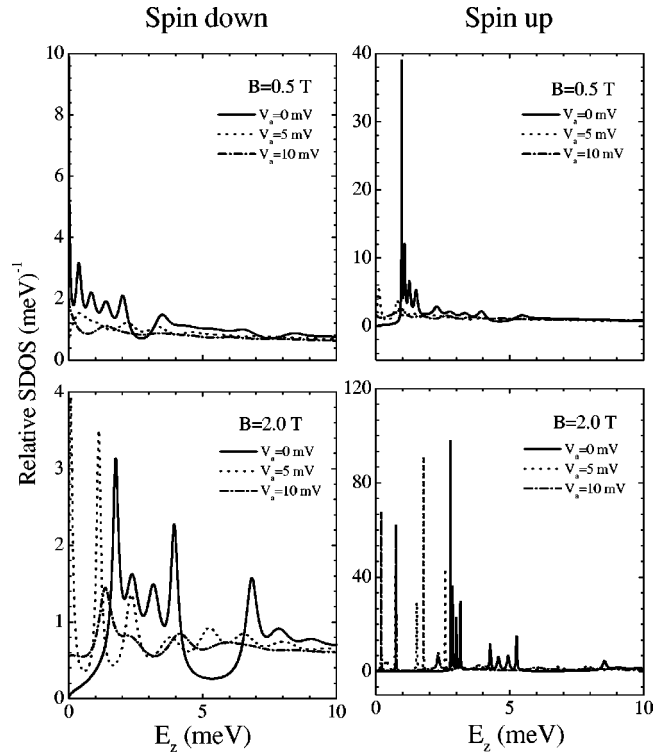
FIG. 6. The relative SDOS distribution within one ZnSe/$Zn_{1-x}Mn_x$Se spin superlattice at zero bias and under two fixed applied biases $V_a = 5, 10$ mV. $L_1 = 20$ nm, $L_2 = 10$ nm, $L_3 = 10$ nm, $B = 0.5, 2$ T.
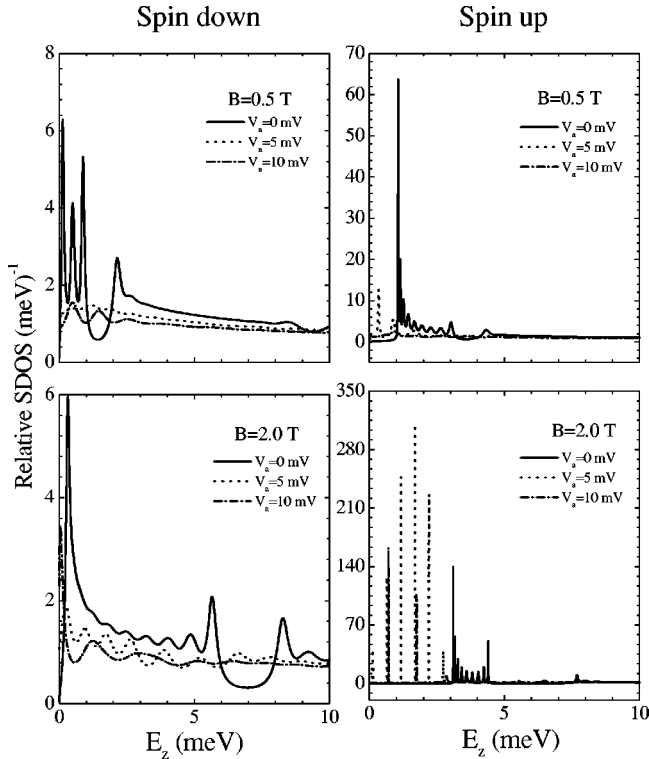
FIG. 5. The relative SDOS distribution within one ZnSe/$Zn_{1-x}Mn_x$Se spin superlattice at zero bias and under two fixed applied biases $V_a = 5, 10$ mV. $L_1 = 20$ nm, $L_2 = 10$ nm, $B = 0.5, 2$ T.

lations are larger. With increasing the external magnetic field, SDOS increases, the magnitudes of the SDOS oscillations increase, thus the states become more localized. Moreover, at zero bias or under a smaller bias, the total number of peaks in each oscillation SDOS band is exactly the same as that of resonant peaks in each corresponding transmission band. The systems with different configurations also exhibit quite different distributions of states. Under an applied bias, the corresponding SDOS distributions over the superlattice differ essentially from those for zero bias case. The magnitudes of oscillations decrease and SDOS spectra are smoothed out.

Figure 7 shows the current density as the function of the applied bias under two fixed magnetic fields $B = 0.5, 2$ T. One can see that under a smaller magnetic field, both the spin-down component and spin-up component of the current density display weak oscillations and weak negative differential resistances. This behavior is a direct consequence of the resonance in $T_{\downarrow}(E_z, V_a, B)$ and relatively shallow wells or relatively low barriers in the corresponding superlattice. As the size of the superlattice increases, the spin-down current density increases while the spin-up current density decreases, which results in larger diversity between the spin-down component and spin-up component of the current density. The thicker the corresponding superlattice, the higher is the degree of the spin polarization. Splitting indeed occur for the current density. In contrast with the transmission coefficient, the number of oscillations in the current density spectra has no simple direct correspondence to the number of unit cells. It is hardly to sum up a simple rule to describe its main
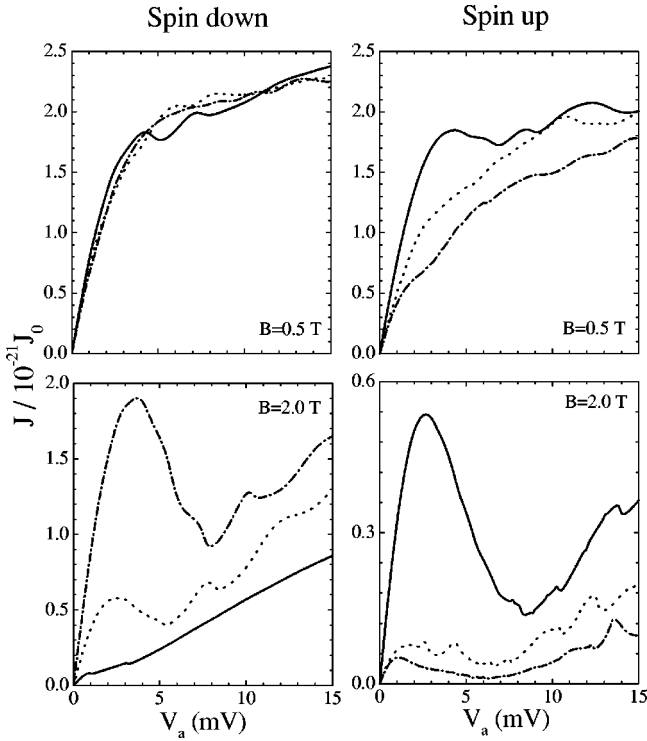
FIG. 7. Spin-dependent current densities as functions of the applied bias for electrons traversing three different configurations of ZnSe/Zn$_{1-x}$Mn$_x$Se spin superlattices. $E_f = 5$ meV. Solid line: $L_1 = L_2 = 10$ nm; dotted line: $L_1 = 20$ nm, $L_2 = 10$ nm; dash-dotted line: $L_1 = 20$ nm, $L_2 = 10$ nm, and $L_3 = 10$ nm.

FIG. 8. Spin-dependent current densities and their respective derivatives as functions of the magnetic field for electrons traversing three different configurations of spin superlattices. Solid line: $L_1 = L_2 = 10$ nm; dotted line: $L_1 = 20$ nm, $L_2 = 10$ nm; dash-dotted line: $L_1 = 20$ nm, $L_2 = 10$ nm, and $L_3 = 10$ nm.

feature. $(N-1)$-fold splitting for n-barrier tunneling no longer holds for the current density in electric superlattices. The oscillations of the current density spectrum at high magnetic field become more irregular. The current density vary nonmonotonously with increasing of the applied bias. Under a high magnetic field, sp-d interaction introduce deeper wells for spin-down electrons and higher barriers for spin-up electrons. Therefore, we can see obvious negative differential resistances. Consequently, the difference between spin-up case and spin-down case is further enlarged, thus the degree of the spin polarization is raised.

Figure 8 shows curves of $J_\uparrow(B, V_a)$ and $J_\downarrow(B, V_a)$, and their respective derivatives, as a function of B. It is shown that the spin-down component of the current density displays both oscillatory behavior and the decay as the magnetic field increases, while the spin-up current density is structureless and exponentially suppressed. These behavior is originated from the tunneling feature of $T_\downarrow$ and $T_\uparrow$. For electron tunneling through the superlattice with a larger size, the spin-down component of the current density is larger than that for electron tunneling through the superlattice with a smaller size, while the spin-up component is quite the contrary. Moreover, the derivatives of the current density $J_\uparrow(B, V_a)$ and $J_\downarrow(B, V_a)$ present rich fine structures, and the derivatives of $J_\downarrow$ show rapid oscillations and have more dips.

In order to further reveal the spin-filtering effect, in Figs. 9 and 10 we present the spin polarization for electrons traversing the three different configurations of the superlattices

as functions of the applied bias and the magnetic field, respectively. It is easily seen that not only the external (electric and magnetic) fields but also the size of the corresponding superlattice greatly change the polarization status of the tunneling electrons. The larger the magnetic field, the higher is the degree of the polarization. At a fixed magnetic field, the polarization shows fine oscillations as functions of the applied bias, and the global trend of the polarization decreases as the electric field increases. However, for electron tunneling through the superlattice with a larger size, the spin polarization can be larger in relatively wide range of the bias for $B > 2$ T, i.e., the total current density is dominated by the spin-down component for $B > 2$ T. The results imply that the spin superlattice with a large size possess stronger spin filtering.

IV. CONCLUDING REMARKS

In summary, we adopt the tight-binding model and the real space Green's function method to investigate spin resonant splitting in the magnetically modulated ZnSe/Zn$_{1-x}$Mn$_x$Se superlattice. The aim of this paper is twofold. On one hand, we explore the external magnetic field, the electric field, and the structural configuration effects on spin-filtering in semimagnetic semiconductor superlattices. On the other hand, the ZnSe/Zn$_{1-x}$Mn$_x$Se spin superlattice may be one of ideal system, through which similarities and differences of splitting features between in multiple-well system and in multiple-barrier system can be considered simul-
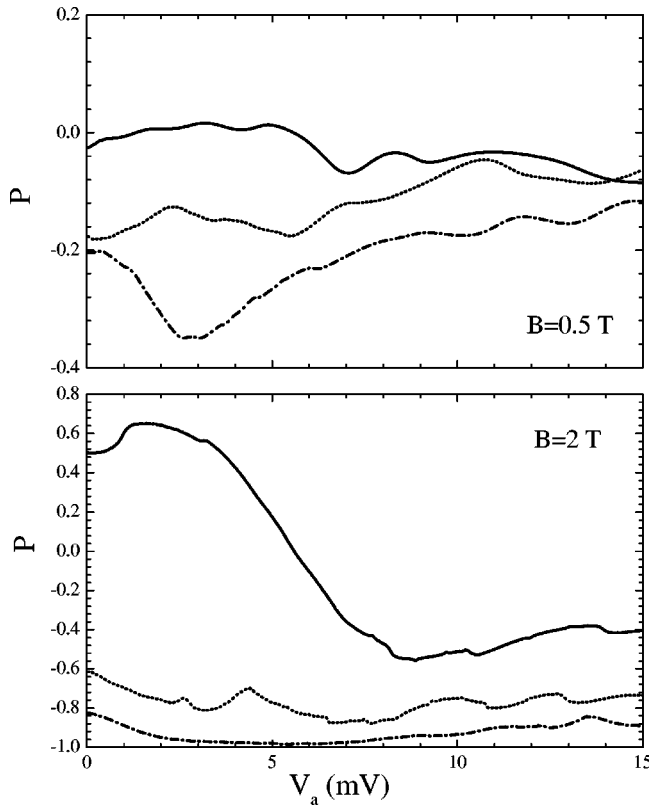
FIG. 9. Spin polarization as functions of the applied bias for electrons traversing three different configurations of spin superlattices. Solid line: $L_1 = L_2 = 10$ nm; dotted line: $L_1 = 20$ nm, $L_2 = 10$ nm; dash-dotted line: $L_1 = 20$ nm, $L_2 = 10$ nm, and $L_3 = 10$ nm.

FIG. 10. Spin polarization as functions of the magnetic field for electrons traversing three different configurations of spin superlattices. Solid line: $L_1 = L_2 = 10$ nm; dotted line: $L_1 = 20$ nm, $L_2 = 10$ nm; dash-dotted line: $L_1 = 20$ nm, $L_2 = 10$ nm, and $L_3 = 10$ nm.

taneously. Numerical results indicate that for electron tunneling through multiple-barrier system, resonant splitting rules of the transmission are exactly the same as that through multiple-well system, that is, at zero bias or under a very small bias, $(n-1)$-fold splitting in the transmission occurs in n-identical wells or in n-identical barriers system. For the current density, the splitting indeed occur, however, it is too complex to sum up a simple rule to describe its main feature. Numerical results further indicate that the degree of polarization can be enhanced by increasing the size of the corresponding structure. The results also show that as the magnetic field increases, the degree of electron polarization is
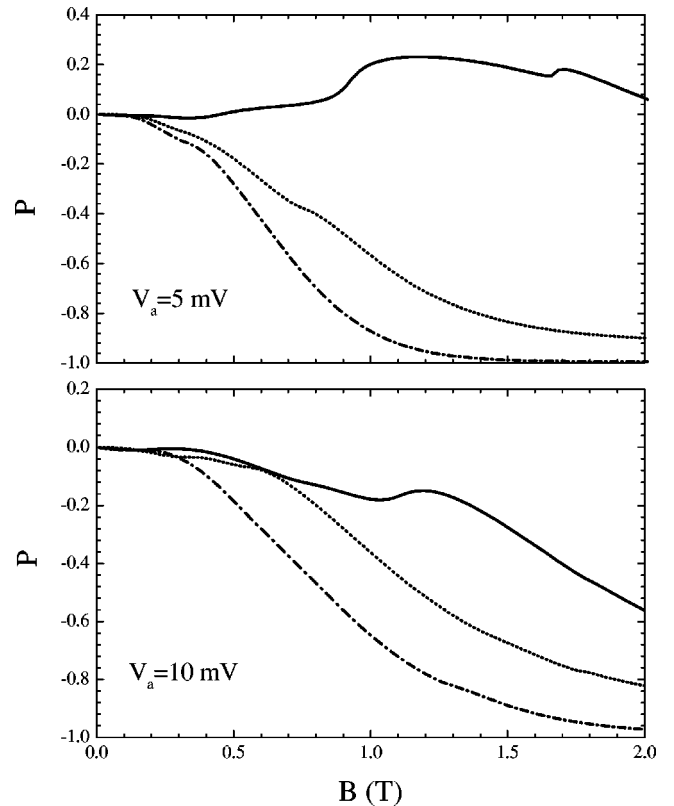
raised. Moreover, it is confirmed that the external electric field can greatly change the splitting rule for both the transmission coefficient and the current density.

[1] G. A. Prinz, Phys. Today **48**, 58 (1995); G. A. Prinz, Science **282**, 1660 (1998).

[2] D. P. DiVincenzo, Science **270**, 255 (1995); B. E. Kane, Nature (London) **393**, 133 (1998).

[3] J. M. Kikkawa, I. P. Smorchkova, N. Samarth, and D. D. Awschalom, Science **277**, 1284 (1997).

[4] D. J. Monsma, R. Vlutters, and J. C. Lodder, Science **281**, 407 (1998).

[5] I. Žutić and S. D. Sarma, Phys. Rev. B **60**, R16 322 (1999).

[6] S. Datta and B. Das, Appl. Phys. Lett. **56**, 665 (1990).

[7] L. Viña, J. Phys.: Condens. Matter **11**, 5929 (1999).

[8] S. Gardelis, C. G. Smith, C. H. W. Barnes, E. H. Linfield, and D. A. Ritchie, Phys. Rev. B **60**, 7764 (1999).

[9] Y. Guo, B.-L. Gu, Z. Zeng, J.-Z. Yu, and Y. Kawazoe, Phys. Rev. B **62**, 2635 (2000).

[10] J. M. D. Teresa, A. Barthélémy, A. Fert, J. P. Contour, F. Montaigne, and P. Seneor, Science **286**, 507 (1999).

[11] M. E. Flatté and J. M. Byers, Phys. Rev. Lett. **84**, 4220 (2000).

[12] J. König, H.-H. Lin, and A. H. MacDonald, Phys. Rev. Lett. **84**, 5628 (2000).

[13] S. A. Crooker, E. Johnston-Halperin, D. D. Awschalom, R. Knobel, and N. Samarth, Phys. Rev. B **61**, R16 307 (2000).

[14] M. Sharma, S. X. Wang, and J. H. Nickel, Phys. Rev. Lett. **82**, 616 (1999).

[15] I. P. Smorchkova, N. Samarth, J. M. Kikkawa, and D. D. Awschalom, Phys. Rev. Lett. **78**, 3571 (1997).

[16] M. V. Ortenberg, Phys. Rev. Lett. **49**, 1041 (1982).

[17] N. Dai, H. Luo, F. C. Zhang, N. Samarth, M. Dobrowolska, and J. K. Furdyna, Phys. Rev. Lett. **67**, 3824 (1991).

[18] W. C. Chou, A. Petrou, J. Warnock, and B. T. Jonker, Phys. Rev. Lett. **67**, 3820 (1991).

[19] V. I. Sugakov and S. A. Yatskevich, Sov. Tech. Phys. Lett. **18**, 134 (1992).

[20] J. C. Egues, Phys. Rev. Lett. **80**, 4578 (1998).

[21] Y. Guo, H. Wang, B.-L. Gu, and Y. Kawazoe, J. Appl. Phys. **88**, 6614 (2000).

[22] Y. Guo, B.-L. Gu, H. Wang, and Y. Kawazoe, Phys. Rev. B **63**, 214415 (2001).

[23] R. Fiederling, M. Keim, G. Reuscher, W. Ossau, G. Schmidt, A. Waag, and L. W. Molenkamp, Nature (London) **402**, 787 (1999).

[24] Y. Ohno, D. K. Young, B. Beschoten, F. Matsukura, H. Ohno, and D. D. Awschalom, Nature (London) **402**, 790 (1999).

[25] B. T. Jonker, Y. D. Park, B. R. Bennett, H. D. Cheong, G. Kioseoglou, and A. Petrou, Phys. Rev. B **62**, 8180 (2000).

[26] R. Fitzgerald, Phys. Today **53**, 21 (2000).

[27] T. Dietl, H. Ohno, F. Matsukuru, J. Cibert, and D. Ferrand, Science **287**, 1019 (2000).

[28] I. Malajovich, J. J. Berry, N. Samarth, and D. D. Awchalom, Nature (London) **411**, 770 (2001).

[29] R. Tsu and L. Esaki, Appl. Phys. Lett. **22**, 562 (1973).

[30] X.-W. Liu and A. P. Stamp, Phys. Rev. B **47**, 16 605 (1993).

[31] X.-W. Liu and A. P. Stamp, Phys. Rev. B **50**, 1588 (1994).

[32] Y. Guo, B.-L. Gu, Z.-Q. Li, Q. Sun, and Y. Kawazoe, Eur. Phys. J. B **3**, 257 (1998).

[33] Y. Guo, B.-L. Gu, Z.-Q. Li, J.-Z. Yu, and Y. Kawazoe, J. Appl. Phys. **83**, 4545 (1998).

[34] Z. Y. Zeng, L. D. Zhang, X. H. Yan, and J. Q. You, Phys. Rev. B **60**, 1515 (1999).

[35] A. Aldea, P. Gartner, and I. Corcotoi, Phys. Rev. B **45**, 14 122 (1992).

[36] J. K. Furdyna, J. Appl. Phys. **64**, R29 (1988).